Influence of Electron Interactions on Metallic Properties. I. Specific Heat*

S. D. Silverstein†‡

University of Illinois, Urbana, Illinois

(Received May 24, 1962)

The specific heat of an intermediate density electron gas has been calculated by the use of a momentum-transfer interpolation procedure analogous to that used by Nozières and Pines in the calculation of the correlation energy. The explicit momentum transfer dependence of the derivative of the self-energy at the Fermi surface has been calculated in the long-wavelength limit by the use of the random-phase approximation, and in the short-wavelength limit by the use of second-order perturbation theory with the neglect of parallel-spin interactions. The contributions from the intermediate momentum-transfer interactions are determined by a smooth interpolation between the short- and long-range regions. The results obtained by this procedure are in excellent accord with the high-density results for $r_s \sim 1$, and in their application to the alkali metals predict the experimentally observed enhancement of the specific heat ratio.

I. INTRODUCTION

IT has long been assumed that the low-temperature specific heat of an interacting fermion system could be obtained from a knowledge of the single-particle excitation spectrum in the immediate vicinity of the Fermi surface. The essential assumption which is required is that the fermion system be "normal," in that there is a one-to-one correspondence between the excited states of the interacting system to those of the noninteracting system. This assumption is at the heart of Gell-Mann's[1] calculation of the specific heat of a dense electron gas, and Landau's[2] theory of a Fermi liquid. A mathematical justification of such an approach, with the assumption of the validity of perturbation theory has been given by Luttinger.[3]

One is led by these arguments to view the low-lying excitations of the electron gas as those appropriate to a gas of independent quasi-particles which obey Fermi-Dirac statistics. The quasi-particles may be thought of as individual electrons (or holes) plus their associated polarization clouds. Consequently, the low-temperature specific heat is given by the standard linear temperature relation,

$$C_V = \frac{P_F^2 k_b^2 T}{3\hbar^3}\left[\frac{P_F}{m}+\left(\frac{\partial\Sigma(p)}{\partial p}\right)_{p=P_F}\right]^{-1}. \quad (1.1)$$

The self-energy, $\Sigma(p)$, reflects the modification in the energy of the individual particles due to the interaction with the medium; k_b is Boltzmann's constant, and P_F is the Fermi momentum. It is convenient to express the specific heat as the ratio of the interacting value C, to the Sommerfeld free electron value, C_0;

$$C/C_0 = \left[1+\frac{m}{P_F}\left(\frac{\partial\Sigma(p)}{\partial p}\right)_{p=P_F}\right]^{-1}. \quad (1.2)$$

Historically, the necessity of an appropriate account of the effects of Coulomb correlations on the specific heat was made apparent when Bardeen[4] showed that the Hartree-Fock approximation predicted a vanishing density of states at the Fermi surface and an altered temperature dependence of the form $T/\ln T$; a result in contradiction with experiment.

A calculation of the correlation effects was made by Pines[5] on the basis of the Bohm-Pines[6] collective theory of the electron gas. He calculated the specific heat by only considering the effect of the exchange contribution arising from the short-range part of the Coulomb interaction. The justification for such treatment was the fact that the collective plasma oscillations are the dominant low momentum (or correspondingly long wavelength) elementary excitations of the electron gas. Under ordinary conditions there is insufficient energy to excite one of these collective modes. Thus, the low-momentum-transfer Coulomb interactions which describe the coupling between electrons and collective oscillations are effectively "frozen out" for wave vectors $k \lesssim k_c$; k_c corresponds to the maximum wave vector for which the plasmons constitute an independent mode of the elementary excitations. The results of Pines are approximate in that he neglected contributions to the quasi-particle energy from higher-order terms in the short-range interaction and from the screened long-range interaction.

Gell-Mann obtained the specific heat in the random phase approximation (RPA) by an appropriate generalization of the Gell-Mann, Brueckner[7] technique for the evaluation of the correlation energy. His resulting expansion in the density parameter[8] r_s is:

$$C/C_0 = [1 - 0.083 r_s(\ln r_s + 0.203) + \cdots]^{-1}. \quad (1.3)$$

[1] M. Gell-Mann, Phys. Rev. **106**, 369 (1957).
[2] L. D. Landau, Soviet Phys.—JETP **3**, 920 (1957).
[3] J. M. Luttinger, Phys. Rev. **121**, 942 (1961)
[4] J. Bardeen, Phys. Rev. **50**, 1098 (1936).
[5] D. Pines, Phys. Rev. **92**, 626 (1953).
[6] D. Bohm and D. Pines, Phys. Rev. **92**, 609 (1953).
[7] M. Gell-Mann and K. A. Brueckner, Phys. Rev. **106**, 364 (1957).

[8] The density is represented in units of the dimensionless parameter r_s, where $n^{-1} = 4\pi/3(a_0 r_s)^3$, a_0 being the Bohr radius. The Fermi momentum P_F becomes $1/\alpha a_0 r_s$, where $\alpha = (4/9\pi)^{1/3}$. It subsequently proves convenient to work in units where momentum and energy are expressed in units of the Fermi momentum and twice the Fermi energy.

FIG. 1. The graphical representation of the RPA self-energy process. The dashed and wavy lines correspond to the bare Coulomb interaction $-iV(q)$, and the screened Coulomb interaction $-iV(q)/\epsilon(q,u)$. The single lines correspond to free electron hole propagators.

Quinn and Ferrell,[9] in a subsequent calculation, used field-theoretic techniques to obtain the same high-density expansion. DuBois,[10] using similar methods, succeeded in calculating the next order in the r_s expansion. The net results, although extremely useful in a pedagogical sense, are restricted to densities $r_s \lesssim 1$ and thus do not apply to the intermediate r_s region of metallic densities, $(2 \lesssim r_s \lesssim 6)$.

A calculation aimed at the intermediate density region has been given by Fletcher and Larson.[11] Their work consisted of an extension to second order of the previously discussed calculation of Pines. Metallic properties were then calculated solely on the basis of the short-range, large-momentum-transfer interactions. As will be shown, their results suffer from the neglect of long-range interactions and from the inadequacy of second-order perturbation theory for momentum transfers in the region of the plasmon cutoff k_c.

The purpose of our calculation is to obtain the electronic specific heat for the intermediate region of metallic densities. We accomplish this by an appropriate extension of the Nozières-Pines[12] interpolation calculation of the correlation energy. That is, we obtain an explicit momentum-transfer dependence of the long- and short-range contributions to the derivative of the self-energy. We assume that the effect of long-range interactions can be described by the RPA; the results for which will be represented in the form

$$\Sigma_{L.R.}'(P_F) = \int_0^{\beta_1 P_F} \sigma_{L.R.}'(q)dq, \qquad (1.4)$$

where Σ' denotes the momentum derivative of the self-energy contribution. The short-range effects will be calculated on the basis of second-order perturbation theory with the neglect of parallel-spin interactions. Likewise, the results will be expressed in the form

$$\Sigma_{S.R.}'(P_F) = \int_{\beta_2 P_F}^{\infty} \sigma_{S.R.}'(q)dq. \qquad (1.5)$$

[9] J. J. Quinn and R. A. Ferrell, Phys. Rev. 112, 812 (1958).
[10] D. E. DuBois, Ann. Phys. (New York) 7, 174 (1959); 8, 29 (1959).
[11] J. G. Fletcher and D. C. Larson, Phys. Rev. 111, 455 (1958).
[12] P. Nozières and D. Pines, Phys. Rev. 109, 762 (1958).

The intermediate momentum-transfer region $(\beta_1 P_F < q < \beta_2 P_F)$ is characterized by an admixture of direct and exchange contributions which, at present, we have no direct means of calculating. Therefore, we indirectly approximate it by a smooth interpolation between the long- and short-range regions. The contribution to the derivative of the self-energy from all interactions is then obtained by a numerical integration of the interpolated $\sigma'(q)$ over all momentum transfers.

The results obtained by this procedure are in accord with the high-density results for $r_s \sim 1$, and in their application to the alkali metals exhibit the experimentally observed enhancement of the specific-heat ratio.

II. CONTRIBUTION TO THE SPECIFIC HEAT FROM DIFFERENT REGIONS OF MOMENTUM TRANSFER

We first wish to determine the contribution of the long-range interactions to the self-energy. It has been shown[12] that the long-range effects, characterized by momentum transfers $q < \beta_1 P_F$, are well described by the RPA. The self-energy expansion within this approximation is indicated by the perturbation diagrams of Fig. 1. From the standard rules for interpreting such diagrams, we obtain

$$\Sigma_{L.R.}(p) = +i \int_{q<\beta_1 P_F} \frac{d^3q\,du}{(2\pi)^4} \left\{ v(q)G_{1<}^0(p+q, \, p^2/2m+u) \right.$$
$$\left. - \frac{v^2(q)}{\epsilon(q,u)} \Pi_0(q,u)G_1^0(p+q; \, p^2/2m+u) \right\}. \qquad (2.1)$$

The terms in this relation are defined as follows:

(a) $v(q)$ is the bare Coulomb propagator, $4\pi^2/q^2$.

(b) $\Pi_0(q,u)$ is the bare polarization propagator coming from the closed loop of the second diagram of Fig. 1.

(c) G_1^0 is the free fermion propagator,

$$G_1^0 = 1/[\omega - p^2/2m + i(1-2n_p)\delta]. \qquad (2.2)$$

(d) $\epsilon(qu)$ is the RPA dielectric constant, which is conveniently expressed in terms of the integral equation for the RPA screened interaction,

$$v(q)/\epsilon(q,u) = v(q) - v^2(q)\Pi_0(q,u)/\epsilon(q,u). \qquad (2.3)$$

(e) $G_{1<}^0$ corresponds to the nonpropagating fermion line in the first diagram of Fig. 1. This form is obtained from the Wick contraction of the first interaction term in the standard S matrix expansion of the single-particle Green's function. The frequency integral of this function is given by

$$\int \frac{d\omega}{2\pi} G_{1<}^0(p,\omega) = -in_p. \qquad (2.4)$$

By making use of (2.3), we can re-express the self-energy in the more convenient form

$$\Sigma_{\text{L.R.}}(p) = -\int_{q<\beta_1 P_F} \frac{d^3q}{(2\pi)^3} v(\mathbf{q}) + i$$

$$\times \int_{q<\beta_1 P_F} \frac{d^3q\, du}{(2\pi)^4} \frac{v(\mathbf{q})}{\epsilon(\mathbf{q}u)} G_1^0(\mathbf{p}+\mathbf{q};p^2/2m+u). \quad (2.5)$$

The first term on the right side of (2.5) is independent of the quasi-particle momentum. Thus, it will not contribute to the density of states and need not concern us further. Converting to r_s units,[8] we express the contributing part of the self-energy, in rydberg units, in the form

$$\Sigma_{\text{L.R.}}(p) = \frac{i}{2\pi^3\alpha r_s} \int_{q<\beta_1} \frac{d^3q}{q^2}$$

$$\times \int_{-\infty}^{+\infty} du \frac{G_1^0(\mathbf{p}+\mathbf{q};p^2/2m+u)}{\epsilon(\mathbf{q},u)}. \quad (2.6)$$

We wish to evaluate this integral by contour integration. Therefore, we must first investigate the analytic properties of the integrand. The real and imaginary parts of the RPA dielectric constant are given by

$$\text{Re}\,\epsilon_{\text{RPA}}(\mathbf{q},u)$$

$$= 1 - \frac{2\alpha r_s}{\pi^2 q^2} \int_{p<1} d^3p \frac{\mathbf{q}\cdot(\frac{1}{2}\mathbf{q}+\mathbf{p})}{u^2 - [\mathbf{q}\cdot(\mathbf{q}/2+\mathbf{p})]^2}, \quad (2.7a)$$

and

$$\text{Im}\,\epsilon_{\text{RPA}}(\mathbf{q},u) = \frac{\alpha r_s}{\pi q^2} \int_{p<1<|\mathbf{p}+\mathbf{q}|} d^3p \{\delta(u-\mathbf{q}\cdot(\tfrac{1}{2}\mathbf{q}+\mathbf{p}))$$

$$+\delta(u+\mathbf{q}\cdot(\tfrac{1}{2}\mathbf{q}+\mathbf{p}))\}. \quad (2.7b)$$

In the long-wavelength limit, the RPA dielectric constant will have zeros corresponding to the solutions of the plasmon dispension relation. These solutions appear in the second and fourth quadrants of the complex u plane, where the displacement from the real axis approaches zero in the long-wavelength limit. We represent these solutions by

$$u = \pm\omega_p[1+f(q)]\mp i\delta. \quad (2.8)$$

The plasma frequency ω_p, as expressed in our units, assumes the form $\omega_p^2 = 4\pi\alpha r_s/3$. Furthermore, the mapping of $\epsilon(q,u)$ into the complex u plane will exhibit cuts extending to $\pm(\frac{1}{2}q^2+q)\mp i\delta$. Finally, taking into account the poles of G_1^0, we indicate the mapping of the total integrand of (2.6) and the contour chosen for the integration in Fig. 2. For reasons of clarity the $i\delta$ factors have been chosen to displace the singularities rather than to prescribe the equivalent deformation of the contour. Moreover, we are interested in the self-energies for which $p > P_F$; hence, we only have the
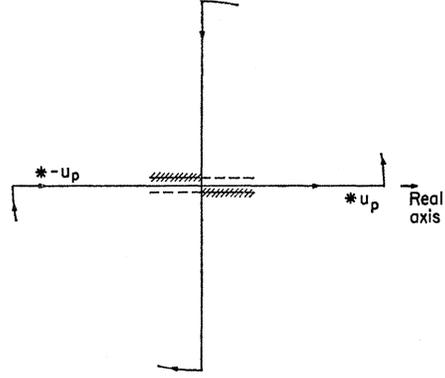
FIG. 2. The mapping of the function $G_1^0(\mathbf{p}+\mathbf{q}, p^2/2m+u)/\epsilon(\mathbf{q},u)$ in the complex u plane. The arrows indicate the contour chosen.

contributions from the G_1^0 singularity which lies in the third quadrant. In a manner analogous to Quinn and Ferrell, the results of the contour integration can be expressed in the form

$$\Sigma(p) = \Sigma_{\text{line}}(p) + \Sigma_{\text{res}}(p), \quad (2.9)$$

where

$$\Sigma_{\text{res}}(p) = \frac{1}{\pi^2\alpha r_s} \int_{p>|\mathbf{p}+\mathbf{q}|>1,\,q<\beta_1} d^3q \frac{1}{q^2\epsilon(\mathbf{q},\,\mathbf{q}\cdot(\frac{1}{2}\mathbf{q}+\mathbf{p}))}, \quad (2.10)$$

and

$$\Sigma_{\text{line}}(p) = \frac{-i}{2\pi^3\alpha r_s} \int_{q<\beta_1} \frac{d^3q}{q^2}$$

$$\times \int_{-i\infty}^{+i\infty} du \frac{G_1^0(\mathbf{p}+\mathbf{q}, p^2/2m+u)}{\epsilon(\mathbf{q},u)}. \quad (2.11)$$

The derivatives of the residue and the line integral terms yield the contributions from the transitions along and across the Fermi surface, respectively. This breakup can be obtained by following DuBois' procedure of differentiating the self-energy prior to the frequency integration. The residue contribution as shown by Quinn and Ferrell yields the high-density limit of Gell-Mann. DuBois used both contributions to obtain the next order in the r_s expansion. In these procedures, the momentum transfer was limited to values of $q < 1$ and the functional dependence of q was not retained. Our treatment differs in that a momentum-transfer interpolation procedure requires an explicit q dependence.

Considering the residue term first, we obtain, upon transformation of the momentum restrictions into the appropriate integration limits,

$$\Sigma_{\text{res}}(p) = \frac{2}{\pi\alpha r_s} \int_0^{\beta_1} dq \int_{-1}^{-q/2p} dx \frac{1}{\epsilon(q, \frac{1}{2}q^2+qpx)}$$

$$- \frac{2}{\pi\alpha r_s} \int_{p-1}^{\beta_1} dq \int_{-1}^{(1-p^2-q^2)/2pq} dx \frac{1}{\epsilon(q, \frac{1}{2}q^2+qpx)}. \quad (2.12)$$

Expanding about the Fermi surface and taking the derivative, we obtain

$$\Sigma_{\text{res}}'(1) = \frac{2}{\pi\alpha r_s}\int_0^{\beta_1}\frac{dq}{q\epsilon(q,0)}, \qquad (2.13)$$

where $\epsilon(q,0)$ is the static dielectric constant,

$$\epsilon(q,0) = 1 + \frac{2\alpha r_s}{\pi q^2}\left[1 + \frac{(1-\frac{1}{4}q^2)}{2q}\ln\left|\frac{1+\frac{1}{2}q}{1-\frac{1}{2}q}\right|\right]. \quad (2.14)$$

It is convenient in the evaluation of the line integral contribution to transform variables $u \rightarrow iqu$. Furthermore, since the line integral contribution is real,[9] we can re-express (2.11) in the form

$$\Sigma_{\text{line}}(p) = \frac{2}{\pi^2\alpha r_s}\int_0^{\beta_1}dq\int_0^\infty\frac{du}{\epsilon(q,iqu)}$$

$$\times\int_{-1}^{+1}dx\,\frac{\frac{1}{2}q+px}{(\frac{1}{2}q+px)^2+u^2}. \quad (2.15)$$

The angular integration yields

$$\int_{-1}^{+1}dx\,\frac{\frac{1}{2}q+px}{(\frac{1}{2}q+px)^2+u^2} = \frac{q}{u^2+p^2}+O(q^3). \quad (2.16)$$

We will express the long-range contribution as a power series expansion in the momentum transfer for which we retain only the leading terms. Hence, the higher-order effects from the angular integration will be neglected. Therefore,

$$\Sigma_{\text{line}}(p) \approx \frac{2}{\pi^2\alpha r_s}\int_0^{\beta_1}qdq\int_0^\infty\frac{du}{(p^2+u^2)\epsilon(q,iqu)}. \quad (2.17)$$

For small q, $\epsilon(q,iqu)$ can be approximated by

$$\epsilon(q,iqu) \approx 1 + \frac{4\alpha r_s}{\pi q^2}\left[\left(1-u\tan^{-1}\frac{1}{u}\right)+\frac{q^2}{2(1+u^2)^2}\right]. \quad (2.18)$$

We substitute (2.18) into (2.17) and perform an expansion of the total integrand in powers of the momentum transfer q. We then take the derivative at the Fermi surface and evaluate the coefficient by numerical integration. The result is expressed by

$$\Sigma_{\text{line}}'(1) = -\int_0^{\beta_1}dq\left[\frac{3.37}{\pi(\alpha r_s)^2}q^3+O(q^5)\right]. \quad (2.19)$$

The total long-range contribution to the derivative of the quasi-particle self-energy, through terms of order β_1^4, is given by the sum of (2.19) and (2.13). Therefore, $\sigma_{\text{L.R.}}'(q)$, as defined by (1.4), assumes the form

$$\sigma_{\text{L.R.}}'(q) \underset{q<\beta_1}{\approx} \left[\frac{q}{2(\alpha r_s)^2}-\frac{q^3}{(\alpha r_s)^2}\left(\frac{1}{4}+\frac{\pi}{8\alpha r_s}+\frac{3.37}{\pi}\right)\right]. \quad (2.20)$$

FIG. 3. First- and second-order self-energy diagrams.

We see from the above that the behavior of the extreme low-momentum-transfer region is primarily governed by the residue contribution, which has been traced physically to the effect of transitions along the Fermi surface. However, as q increases, the perpendicular transitions in the specific-heat process become more important. In the realm of intermediate r_s, the perpendicular transitions are the dominant contribution to the q^3 term. This effect imposes a large negative curvature on $\sigma_{\text{L.R.}}'(q)$, a result which is quite important in that it allows us to perform a sensible interpolation with the contributions arising from the high-q region.

We now study the short-range contributions. On the basis of physical considerations, we would expect the short-range interactions to be primarily restricted to electrons of antiparallel spin. That is, repulsive forces due to the Pauli exclusion principle prevent electrons of the same spin from getting too close to each other. These considerations are substantiated by an examination of the second-order perturbation diagrams, Fig. 3. The contribution from diagram (a) is identically zero. This physically corresponds to the fact that a sharp Fermi surface prohibits an electron and a hole from being in the same state. The contribution from (b) involves both parallel and antiparallel spin intermediate states, while (c) has all internal fermion lines connected and thus only involves states of parallel spin. For large q we can make the approximation

$$\lim_{q\text{ large}} v(\mathbf{q}+\mathbf{p}-\mathbf{p}_1) \approx v(\mathbf{q}). \quad (2.21)$$

In the region for which the above approximation is applicable, we see that the contribution of (c) will effectively cancel against one-half of that of (b).

There is, however, some ambiguity as to the minimum value of q for which (2.21) remains a reasonable approximation. Fletcher and Larson, who calculated the specific heat solely on the basis of the short-range interactions, extended the approximation down to the maximum RPA radius of convergence, $q_c = 0.47r_s^{1/2}$. This approximation does not seem entirely justified for momentum transfers at or below the Fermi momentum.

We consider the proposal of Nozières and Pines as being more reliable, i.e., that the approximation should be satisfied on the average for momentum transfers greater than 1.5 (in units of Fermi momentum). Then, restricting ourselves to values of $q \geqslant 1.5$, we represent the short-range contribution to the self-energy by

$$\Sigma_{\text{S.R.}}(p,\beta_2) \underset{p>1, \beta_2>1.5}{=} \Sigma^1(p,\beta_2) - \tfrac{1}{2}\Sigma_b{}^2(p,\beta_2), \quad (2.22)$$

where

$$\Sigma^1(p,\beta_2) = -\frac{1}{\pi^2 \alpha r_s} \int_{|p+q|<1, q>\beta_2} \frac{d^3q}{q^2}, \quad (2.23)$$

and

$$
\tfrac{1}{2}\Sigma_b{}^2(p,\beta_2)
$$

$$
= -\frac{1}{2\pi^4}\int_{|p_1-q|<1<p_1, |p+q|<1, \beta_2<q}\int \frac{d^3p_1 d^3q}{q^4 \mathbf{q}\cdot(\mathbf{q}+\mathbf{p}-\mathbf{p}_1)}
$$

$$
- \frac{1}{2\pi^4}\int_{p_1<1<|p_1-q|, 1<|p+q|, \beta_2<q}\int \frac{d^3p_1 d^3q}{q^4 \mathbf{q}\cdot(\mathbf{q}+\mathbf{p}-\mathbf{p}_1)}.
$$

$$(2.24)$$

Exact integrations over intersections of Fermi spheres are straightforward but rather lengthy. In the particular example of (2.24), a simple transformation of variables converts our expression to the integrals considered by Fletcher and Larson. They have evaluated the integrals as a function of the minimum momentum transfer cutoff β_2. Rather than recalculate the integrals we can simply alter their results to obtain the explicit momentum transfer dependence. We find

$$
\sigma_{\text{S.R.}}{}'(q) = -\left\{ \frac{1}{\pi\alpha r_s}\left(\frac{q^2-2}{q}\right) + \frac{1}{\pi^2}\left[-\frac{4}{3q} + \frac{8}{3q^3}(1+\ln 2)\right.\right.
$$

$$
\left. + \left(\frac{1}{12} - \frac{3}{2q^2} + \frac{2}{q^4}\right)\ln\left(\frac{1+\tfrac{1}{2}q}{1-\tfrac{1}{2}q}\right) - \frac{4}{3q^3}\ln(4-q^2)\right.
$$

$$
\left.\left. + \left(\frac{-q}{4} + \frac{7}{6q} - \frac{2}{3q^3}\right)\frac{1}{(1-\tfrac{1}{4}q^2)}\right]\right\}, \quad q<2. \quad (2.25)
$$

For the region $q>2$, the Pauli-principle restrictions are considerably simplified; the second term of (2.24) giving the only contribution. Differentiating and integrating, we find

$$
\sigma_{\text{S.R.}}{}' = \frac{2}{\pi^2 q^3}\left[\left(\frac{2}{3} + q - \frac{q^3}{6}\right)\ln\left(1 + \frac{2}{q}\right) + \left(-\frac{2}{3} + q - \frac{q^3}{6}\right)\right.
$$

$$
\left. \times \ln\left(1 - \frac{2}{q}\right) - \frac{2}{3}q\right], \quad q>2 \quad (2.26)
$$

The forms of $\sigma'(q)$ for the high- and low-momentum transfer regions, given by (2.20), (2.25), and (2.26), are now plotted for values of r_s throughout the region

$1 \leqslant r_s \leqslant 5.6$. We approximate the form of $\sigma'(q)$ for the intermediate momentum transfers by a smooth curve drawn between the long- and short-range regions. The
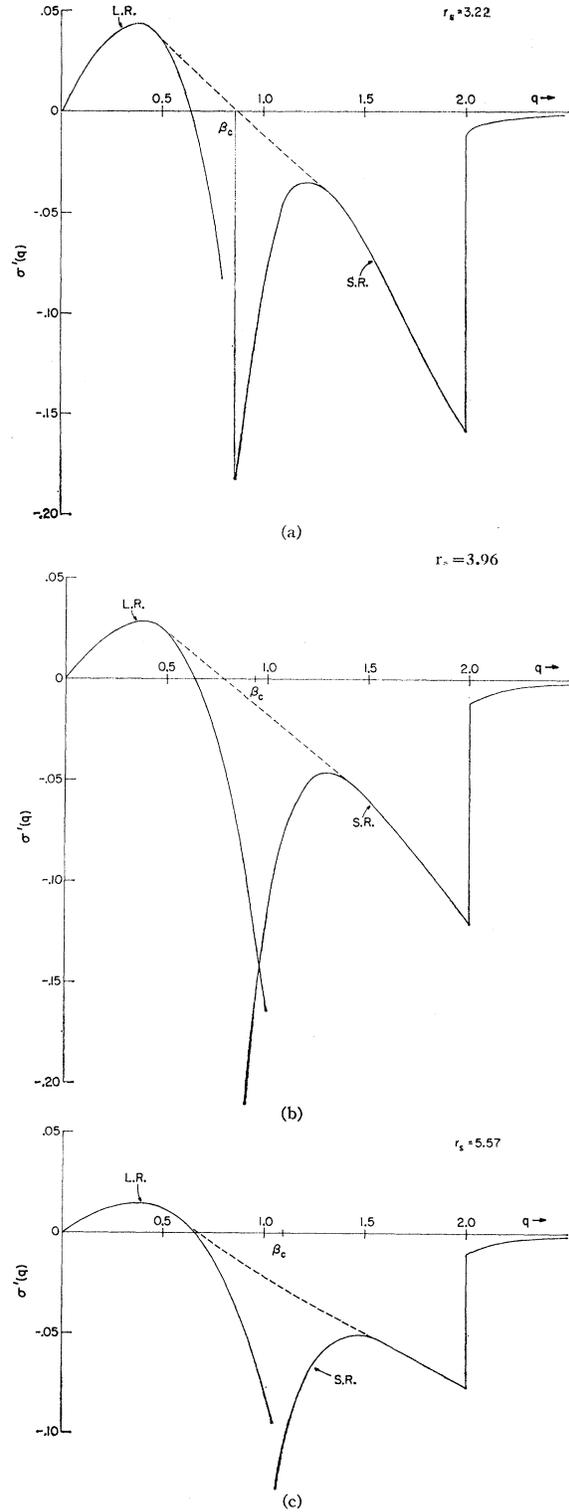
FIG. 4. Sample interpolation curves for different values of r_s.
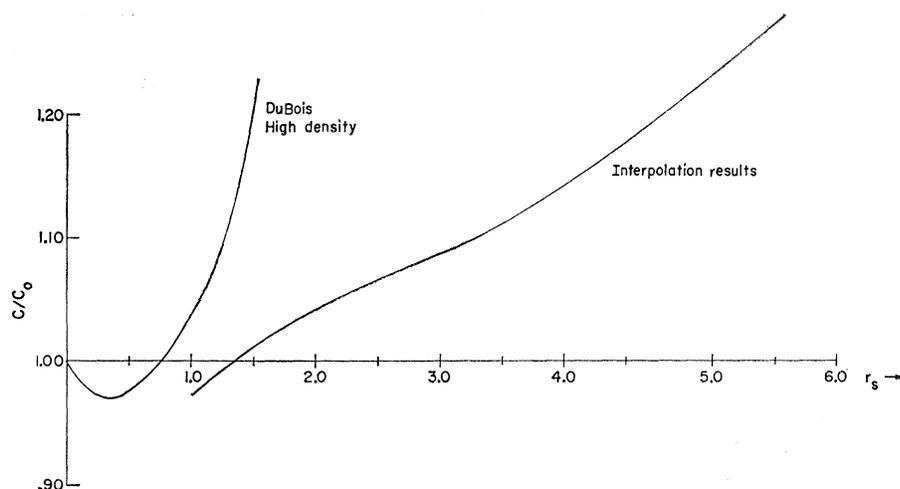
Fig. 5. Plot of C/C_0 as calculated by the interpolation procedure with a comparison to the high-density results of DuBois.

resultant derivative of the self-energy for a given value of r_s is obtained from the numerical integration of $\sigma'(q)$ over all momentum transfers. Specific examples of these are indicated in Fig. 4.

III. RESULTS AND DISCUSSION

In Fig. 5 we have plotted the results obtained for C/C_0 as a function of r_s; we have also indicated the high-density results of DuBois. DuBois estimates that his high-density expansion is accurate for $r_s \lesssim 1$, and further proposes that his results yield an overenhancement of the C/C_0 ratio by as much as 50% at $r_s \sim 2$. Our results, as apparent from Fig. 5, are in excellent accord with the high-density results. We differ in the prediction of the onset of the enhanced ratio; the high-density results give $r_s \sim 0.8$, while we obtain $r_s \sim 1.3$. It appears that the most probable point for this effect to be realized would lie somewhere between these two values.

We now apply our results to the calculation of the specific heat of the alkali metals. In doing so, we follow Pines[13] in estimating the effects of the periodic lattice by the introduction of an isotropic effective mass m^* into the kinetic-energy term. The specific-heat ratio of the alkali metals, which we denote by $(C/C_0)^*$, is represented by

$$(C/C_0)^* = \left[1 + \frac{(\alpha r_s)^2}{2}\frac{m^*}{m}\Sigma'(1)\right]^{-1}. \quad (3.1)$$

The value of $(C/C_0)^*$ for a given density and effective mass can be obtained from the general C/C_0 curve, Fig. 5, by the application of the relation

$$\left(\frac{C}{C_0}\right)^* = \left[1 + \frac{m^*}{m}\left(\frac{1}{C/C_0} - 1\right)\right]^{-1}. \quad (3.2)$$

[13] D. Pines, in Solid State Physics, edited by F. Seitz and D. Turnbull (Academic Press Inc., New York, 1955), Vol. 1, p. 367.

The results obtained for the alkali metals are listed in Table I, where the values obtained by calorimetric experiments are also listed. There we also give the approximate upper limits on the C/C_0 ratios which are obtained from nuclear magnetic resonance data using a procedure suggested by Pines.[13] This method makes use of "interacting Korringa relations." It must be stressed, however, that these relations are valid in only the high-magnetic-field limit and furthermore rely on the assumption that the Bloch states taking part in the spin-lattice relaxation mechanism can be thought of as a gas of completely independent quasi-particles in the vicinity of the Fermi surface. The interacting Korringa relation is given by

$$T_1\left(\frac{\Delta\mathcal{3C}}{\mathcal{3C}}\right) = \frac{\hbar}{4\pi k_b T}\left(\frac{\chi_s}{\chi_0}\right)^2\left(\frac{\gamma_e}{\gamma_n}\right)^2\left(\frac{\rho_0(E_f)}{\rho(E_f)}\right)^2. \quad (3.3)$$

Here T_1 is the spin-lattice relaxation time, $\Delta\mathcal{3C}/\mathcal{3C}$ is the Knight shift, χ_s/χ_0 is the ratio of the actual to the free Pauli electron spin susceptibility, and $\rho_0(E_f)/\rho(E_f)$ represents the ratio of the free to the interacting density of states at the Fermi surface. From a knowledge of χ_s and T_1, one puts an upper limit on the state density

TABLE I. Experimental values and results obtained.

	Li[7]	Na[23]	K[39]	Rb[85]	Cs[133]
r_s	3.22	3.96	4.87	5.18	5.57
m^*/m[a]	1.45	0.98	0.93	0.89	0.83
$(C/C_0)^*$	1.14	1.14	1.19	1.20	1.21
$(C/C_0)_{exp}$ [b]	1.60	1.25	1.18		
T_1 m/sec [c]	150±5	15.9±3			
$(\Delta\mathcal{3C}/\mathcal{3C})\times10^{-2}$	0.0249[d]	0.113[d]		0.653[d]	1.46[d]
$(\chi_s)_{exp}\times10^6$	2.08±0.1[e]	0.89±0.04[f]			
$(C/C_0)_{max}^*$	1.38±0.09	1.11±0.08			

[a] See D. Pines (reference 13).
[b] Calorimetric results with effective-mass corrections as quoted by Fletcher and Larson (reference 19).
[c] D. Holcomb and R. F. Norberg, Phys. Rev. 98, 1074 (1955).
[d] W. D. Knight, Solid State Phys. 2, 93 (1956).
[e] R. T. Schumacher and C. P. Slichter, Phys. Rev. 101, 58 (1956).
[f] R. T. Schumacher and W. E. Vehse, Bull. Am. Phys. Soc. 4, 296 (196

$\rho(E_f)$. The upper-limit condition is due to the fact that other unaccounted for relaxation mechanisms serve to increase the value of T_1. The experimental values and the results obtained are given in Table I.

We find it difficult to determine the exact limit on the accuracy of the interpolation procedure. Besides assuming nature's regularity in the intermediate region, we must also contend with our approximations for both the long- and short-range regions.

In the long-range region, we have explicitly used the RPA. There are, of course, local field corrections to these results; a specific example of one of these is given by the diagram in Fig. 6. The question naturally arises as to what degree these terms enter in the momentum-transfer expansion. In the calculation of the correlation energy, Nozières and Pines found local field corrections in the β^4 term (β being the long-range cutoff). Moreover, they found these corrections to be small in the region of metallic densities. We have not explicitly evaluated these corrections to the density of states (such an analysis entails a calculation similar to DuBois' evaluation of local field corrections with the added difficulty of retaining the explicit momentum-transfer dependence). However, using the same arguments as presented by Nozières and Pines we likewise feel the corrections will be small.

With reference to the short-range interactions, we find it difficult to assess the accuracy of second-order perturbation theory. It is fairly evident that the short-range perturbation expansion parameter will be proportional to r_s divided by a function, $f(\beta_2)$. A determination of the convergence of the perturbation expansion would necessitate the difficult task of evaluating the next order in the perturbation series. We find from an asymptotic consideration of the third-order term that $\beta_2^2/f(\beta_2)$ will be finite in the limit of infinite β_2. These considerations imply that second-order perturbation theory should prove reliable for intermediate r_s as long as one chooses a large enough β_2. These conclusions are further substantiated by an investigation of the shape of the $\sigma_{S.R.}{}'(q)$ curves as plotted for various values of r_s (Fig. 4). We see that the curves follow a normal pattern down to values of momentum transfer which increase with correspondingly increasing values of r_s. The rapid variation in curvature beginning for values of $q \sim 1.3$ can, in part, be attributed to the inadequacy of a second-order result for low momentum transfers.

FIG. 6. An example of a local field correction to RPA self-energy.
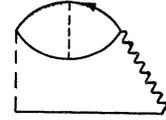
This behavior further suggests that the choice of a minimum cutoff in or below this region is inappropriate for intermediate values of r_s. We conclude, therefore, that the results of Fletcher and Larson are not applicable for $q \lesssim 1.5$. In the interpolation calculation of the correlation energy[12] the estimate of error was $\sim 15\%$. However, our curves indicate that the long- and short-range contributions tend to cancel each other; the results obtained are, therefore, more sensitive to a particular interpolation. An estimate, $\sim 25\%$, is obtained by considering radical deviations from the most obvious intermediate path. This estimate of error in the derivative of the self-energy leads to an estimate of possible errors in the value of C/C_0 of the order of 10%.

The error estimates of $\sim 10\%$ cannot be extended to the quantitative values given for the alkali metals. In this application, one must also contend with the accuracy of the effective mass approximation in compensating for the effects of the periodic lattice, and the fact that our calculations have neglected the effects of electron-phonon corrections. Preliminary investigations[14] indicate that the electron-phonon interaction can serve to increase the effective mass by as much as 20% in the case of Na. This effect is calculated by coherently adding the contribution to the mass renormalization from the electron-phonon interaction. The 20% correction serves as an indication of what might happen rather than a statement of fact. That is, the masses due to electron-electron and electron-phonon interactions certainly do not add coherently, but rather must be reformulated in terms of an over-all net effective interaction.

[14] R. A. Ferrell (private communication).